Stabilizing an Optoelectronic Microwave Oscillator With Photonic Filters

Dmitry Strekalov, David Aveline, *Member, OSA*, Nan Yu, Robert Thompson, Andrey B. Matsko, *Member, OSA*, and Lute Maleki, *Fellow, IEEE, Member, OSA*

Invited Paper

***Abstract*—This paper compares methods of active stabilization of an optoelectronic microwave oscillator (OEO) based on insertion of a source of optical group delay into an OEO loop. The performance of an OEO stabilized with either a high-Q optical cavity or an atomic cell is analyzed. We show that the elements play a role of narrow-band microwave filters improving an OEO stability. An atomic cell also allows for locking the oscillation frequency to particular atomic clock transitions. This reports a proof-of-principle experiment on an OEO stabilization using the effect of electromagnetically induced transparency in a hot rubidium atomic vapor cell.**

***Index Terms*—Atomic clocks, electromagnetically induced transparency, optoelectronic oscillator, photonic filter.**

I. Introduction

MICROWAVE oscillators capable of generating spectrally pure signals at high frequencies are important for a number of applications, including communications, navigation, radar, and precise tests and measurements. Conventional oscillators are based on electronic techniques that employ high quality (Q) factor resonators to achieve high spectral purity. The performance of these oscillators is nevertheless limited by the achievable Qs at room temperature and by the sensitivity of the resonators to environmental perturbations, such as temperature and vibration. High-frequency microwave references may also be obtained by multiplication of signals generated by high quality, but low frequency (MHz), quartz oscillators. The noise associated with the multiplication steps, unfortunately, degrades the performance of the high frequency signals beyond the levels required for high-end applications.

A powerful method of creating high-purity signals is based on techniques of photonics, which are free of some of the intrinsic limitations of ultra-high-frequency electronics mentioned above. In particular, the optoelectronic oscillator (OEO) is a photonic device that produces spectrally pure signals at many tens of gigahertz [1]–[7] limited only by the bandwidth of the modulators and detectors, which currently extends to the 100-GHz range.

In a generic OEO [1] the microwave energy is stored in an optical delay line, eliminating the need for a microwave cavity. However, in this configuration, the long fiber delay line supports many microwave modes imposed on an optical wave. A narrow-band electrical filter should be inserted into the electronic segment of the OEO feedback loop to achieve a stable single-mode operation. The center frequency of this filter determines the operational frequency of the OEO. While this approach yields the desired spectrally pure high-frequency signals, it nevertheless calls for an OEO configuration limited in size by the kilometers of fiber delay needed. Moreover, the long fiber delay is very sensitive to the surrounding environment, so the OEO does not produce an output with high long-term frequency accuracy and stability. The OEO is typically phase locked to a stable reference for long-term stability.

In this paper, we study the properties of the optoelectronic oscillator with either a high-Q optical cavity or an atomic cell, in place of the electronic filter. The first method allows one to choose virtually an arbitrary frequency of oscillation by tuning the cavity. The second method allows one to create a stable frequency reference, especially if the OEO is locked to an atomic clock transition. We theoretically analyze both approaches, and report on a proof-of-principle experiment with the OEO stabilized to the rubidium clock transition with an atomic vapor cell.

We propose to use the effect of electromagnetically induced transparency (EIT) [8]–[10] to stabilize an OEO with an atomic cell. EIT was recently used to produce an ultraslow group velocity of light [11], [12] in atomic vapors [13]–[15] as well as in doped solids [16], [17]. Those results are based on usage of steep frequency dispersion in the vicinity of a narrow EIT resonance. The narrow EIT resonances are applicable for construction of all-optical miniature atomic clocks [18]. We show here that extremely narrow two-photon EIT resonances could also be useful for OEO stabilization.

This paper is organized as follows. We first review the operation of the conventional OEO and then consider configurations with the optical cavity, and the atomic vapor cells. We present the experimental data for the latter case and conclude with a summary.

Manuscript received April 16, 2003; revised August 20, 2003. This work was supported by the National Aeronautics and Space Administration (NASA) under sponsorship of the Defense Advanced Research Projects Agency by the Jet Propulsion Laboratory, California Institute of Technology.

The authors are with the Jet Propulsion Laboratory, California Institute of Technology, Pasadena, CA 91109-8099 USA (e-mail: Andrey.Matsko@jpl.nasa.gov).

Digital Object Identifier 10.1109/JLT.2003.821724

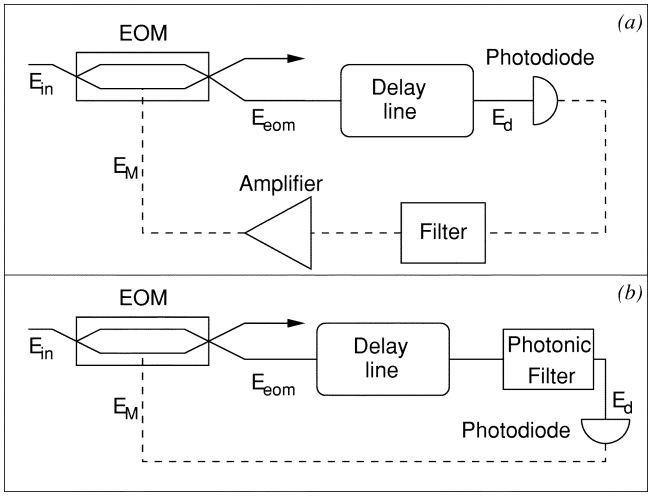

Fig. 1. Optoelectronic oscillator: (a) Usual configuration and (b) configuration with a photonic filter.

II. The Optoelectronic Microwave Oscillator Scheme

The generic scheme of the OEO is shown in Fig. 1(a). Light from a laser is introduced into an electrooptical modulator (EOM). The amplitude-modulated light from the exit port is split with a fiber splitter, with one branch sent into a fiber delay line followed by a photodiode. The other branch provides the optical output of the device. The microwave signal from the output at the photodiode is filtered, amplified, and fed back into the EOM. This system oscillates if the amplification in the closed loop exceeds linear absorption of the loop [1]. The microwave amplifier may be unnecessary to sustain stable oscillations, depending on the power of the laser radiation at the photodetector and the particular features of the modulator and optical delay line.

The fiber delay line is a photonic substitute for a microwave resonator. A longer fiber corresponds to a larger Q-factor. The OEO with such a high-Q photonic storage element is a multimode device, with a dense mode spectrum corresponding to the waves adding in phase as the energy circulates in the loop. A single-mode operation is obtained when a narrow-band microwave filter is inserted in the loop. The filter determines the oscillation frequency, and its stability with respect to environmental perturbations directly determines the stability of the oscillator. While the Q of the filter is not a determining factor for the spectral purity, it nevertheless determines the degree of suppression of all other modes within its passband. The realization of a high-Q microwave filter with center frequency at tens of gigahertz is a complicated task [2].

The microwave filtering may be substituted with photonic methods of spectral purification in the OEO, including either use of several different optical loops [5] or a delay line along with an optical cavity filter. With the latter approach, the oscillation occurs at the frequency of the cavity modes. The spectral purity and the stability are determined either by the time delay in the fiber or by the spectral width of the filter, whichever has the narrowest characteristic linewidth. With such an optical filtering scheme, the OEO becomes an ideal photonic device, where the microwave field is generated without any microwave circuit elements [Fig. 1(b)]. Presently, this realization is hindered by the low efficiency of the EOM, so a microwave amplifier must be included in the OEO loop to provide the needed drive for the modulator.

III. Analysis of the Optoelectronic Oscillator

To find the amplitude and frequency of oscillations, we consider the basic properties of the OEO elements: the fiber delay line, the optoelectronic modulator, and the photodiode.

A. The Electrooptical Modulator

Let us consider an electrooptical modulator of Mach–Zehnder type that transforms a monochromatic radiation $E\exp(i\omega_0 t)$ into amplitude modulated light. The modulator consists of a Mach–Zehnder interferometer with a nonlinear electrooptic crystal placed in an arm. When a microwave field is sent into the crystal, the crystal introduces a time-dependent delay into the arm, and the outgoing light becomes modulated

$$E_{\rm mod}(t) = \frac{1}{2}E(t)\left[1 + e^{i\omega_0(\tau_B + \tau_M(t))}\right] \tag{1}$$

where τ_B is a dc bias delay and $\tau_M(t)$ is the time-dependent delay introduced by the nonlinear crystal given by

$$\tau_M(t) = \xi\frac{L_S}{c}\frac{n_0^3}{2}r_{\rm eff}(E_M(t) + E_M^*(t)). \tag{2}$$

Here the dimensionless parameter ξ ($\xi < 1$) results from the imperfect overlap and phase mismatch of light and microwave fields, L_S is the length of the electrooptic crystal, n_0 is the linear index of refraction of the nonlinear material, and $r_{\rm eff}$ is the coefficient of nonlinearity of the material (e.g., 30 pm/V for $LiNbO_3$).

It is convenient to present the microwave field in the form $E_M(t) + E_M^*(t) = 2\widetilde{E}_M(t)\cos(\omega_M t + \psi(t))$, where $\widetilde{E}_M(t)$ and $\psi(t)$ are slow functions of time. We also write $\tau_M(t) = 2\widetilde{\tau}_M(t)\cos(\omega_M t + \psi(t))$. Then we derive the expressions for the amplitudes of the carrier and the first two sidebands

$$E_{\rm in} = \frac{1}{2}Ee^{-i\omega_0 t}\left[1 + e^{i\omega_0\tau_B}(1 - \omega_0^2\widetilde{\tau}_M^2)\right] \tag{3}$$

$$E_{\pm 1} = \frac{i}{4}E\omega_0\widetilde{\tau}_M e^{-i(\omega_0 \pm \omega_M)t}e^{i\omega_0\tau_B}\left(1 - \frac{1}{2}\omega_0^2\widetilde{\tau}_M^2\right). \tag{4}$$

The description presented above is valid not only for Mach–Zehnder EOMs but also for any kind of EOM. An example is a polarization-based EOM, when a nonlinear medium influencing polarization of the passing light is placed between crossed polarizers, instead of semitransparent mirrors. Such a modulator is used in our experiment discussed in this paper. We should note that some insignificant corrections of the equations should be introduced to describe this modulator; however, for the sake of simplicity, we do not discuss those corrections here.

B. Photodiode

The transformation of light at power $P_{\rm opt}$ into microwaves with power P_{mw} by means of a photodiode is determined by

$$P_{mw} = R^2\rho P_{\rm opt}^2 \tag{5}$$

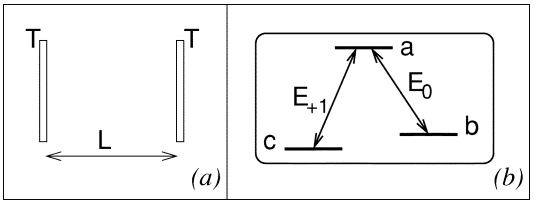

Fig. 2. Group delay lines for OEO stabilization: (a) optical cavity and (b) atomic cell.

where R is a transformation coefficient of the optical power to a photocurrent and ρ is the resistance at the output of the photodiode. The typical values are $R = 0.7$ A/W and $\rho = 50\,\Omega$. We present the complex field amplitude E as

$$|E|^2 = \frac{2\pi P}{\mathcal{A}cn} \tag{6}$$

where P is power, $\mathcal{A}$ is an effective cross-sectional area of the fiber guide, and n is the refractive index of the material. Then, for the amplitude of the microwave field (E_M)

$$E_M = GP_{\rm opt}\Big|_{\omega_M}, \quad G = R\left(\frac{2\pi\rho}{\mathcal{A}_M c}\right)^{1/2} \tag{7}$$

where $P|_{\omega_M}$ is the optical power at the microwave frequency (the power of the optical beat signal) and $\mathcal{A}_M$ is the cross-sectional area of the microwave waveguide.

C. Optical Fiber Delay Line

If one sends monochromatic light with frequency ω_0 into an optical fiber characterized by the effective index of refraction n_0 and length L_f, the output light has a complex electric field amplitude $E_{\rm out}(t)$ that is related to the amplitude of the input light $E_{\rm in}\exp(-i\omega_0 t)$ as

$$E_{\rm out}(t) = \alpha E_{\rm in}\exp(-i\omega_0 t)\exp\left(\frac{i\omega_0 n_0 L_f}{c}\right) \tag{8}$$

where α is the transmission coefficient due to insertion losses and the fiber material and c is the speed of light in the vacuum.

Assuming that the fiber has no dispersion ($n_0(\omega)$ =const) in the range of frequencies we are interested in ($\omega_0 + \Delta\omega \geq \omega \geq \omega_0 - \Delta\omega$), we introduce an effective delay time due to the fiber

$$\tau_f = \frac{n_0 L_f}{c} \tag{9}$$

and, therefore

$$E_{\rm out}(t) = \alpha E_{\rm in}(t - \tau_f). \tag{10}$$

The same expression is valid for a beat-note of any two monochromatic light waves.

IV. Group Delay Lines as Photonic Filters

This section is devoted to a theoretical study of the high-Q optical cavity and the atomic vapor cell (Fig. 2) as photonic filters. The aim is to analyze their suitability for OEO stabilization.

While an optical fiber is a true delay line, which introduces group as well as phase delays, an optical cavity and an atomic cell result in a group delay only. The phase delay of the optical radiation due to these resonant elements is negligibly small. We show that these elements may be effectively treated as microwave filters.

A. A Cavity

Let us consider a cavity consisting of two identical mirrors, with an energy transmission coefficient T ($1 > T > 0$), placed at a distance L from each other Fig. 2(a). The transmission of monochromatic light with a carrier frequency ω_0 through the cavity is characterized by the expression

$$E_{\rm out}(t) = E_{\rm in}\exp(-i\omega_0 t)\frac{T\exp\left(\frac{i\omega_0 L}{c}\right)}{1-\exp\left(\frac{2i\omega_0 L}{c}\right)(1-T)}. \tag{11}$$

It is easy to see from (11) that $E_{\rm out}(t) = \pm E_{\rm in}\exp(-i\omega_0 t)$ if the input wave is resonant with a cavity mode $2\omega_0 L/c = 2\pi m$, where m is an integer.

In an OEO, we deal with a beat-note of light waves; the beat-note frequency ω_M corresponds to the modulation frequency. Let us assume that the pump light $E_{\rm in}$ has frequency ω_0 ($2\omega_0 L/c = 2\pi m + 2\Delta\omega_0 L/c$), and after the modulator the light has a single sideband E_{+1} with frequency $\omega_{+1} = \omega_0 + \omega_M$ ($2\omega_{+1}L/c = 2\pi(m+1) + 2[\Delta\omega_0 + \Delta\omega_M]L/c$). Here $\Delta\omega_0$ and $\Delta\omega_M$ characterize the detunings from the nearest resonance. We derive

$$\begin{aligned} &E^*_{\rm out}(t)E_{+1\ out}(t) \\ &\quad = -E^*_{\rm in}E_{+1}e^{-i\omega_M t} \\ &\qquad \times \frac{T^2 e^{i\Delta\omega_M L/c}}{\left[1-e^{-2i\Delta\omega_0 L/c}(1-T)\right]\left[1-e^{2i(\Delta\omega_0+\Delta\omega_M)L/c}(1-T)\right]}. \end{aligned} \tag{12}$$

For the near resonant fields, this expression transforms to

$$\begin{aligned} &E^*_{\rm out}(t)E_{+1\ out}(t) \\ &\simeq -\frac{T^2 E^*_{\rm in}E_{+1}e^{-i\omega_M t}e^{i\Delta\omega_M L/c}}{\left[\left(T^2+\left(\frac{2\Delta\omega_0 L}{c}\right)^2\right)^2+\left(\frac{2T\Delta\omega_M L}{c}\right)^2\right]^{1/2}} \\ &\qquad \times \exp\left[\frac{\frac{2iT^3\Delta\omega_M L}{c}}{\left(T^2+\left(\frac{2\Delta\omega_0 L}{c}\right)^2\right)^2+\left(\frac{2T\Delta\omega_M L}{c}\right)^2}\right]. \end{aligned} \tag{13}$$

In order to avoid conversion of the frequency fluctuations of the pump laser into amplitude fluctuations, the linewidth of the laser should be much smaller than the width of the optical resonance. If the influence of the laser detunings on the power transmission of light is negligible, (13) may be simplified

$$E^*_{\rm out}(t)E_{+1\ {\rm out}}(t) \approx -E^*_{\rm in}E_{+1}e^{-i\omega_M t}e^{i\Delta\omega_M L(1+2/T)/c}. \tag{14}$$

It is worth mentioning that for $\Delta\omega_0 = 0$, the transmission of the beat-note through the cavity (13) is described by the response function

$$F_c \simeq -\frac{\gamma_c}{\gamma_c - i(\omega_M - \omega_{\rm FSR})} e^{i\pi(\omega_M - \omega_{\rm FSR})/\omega_{\rm FSR}} \tag{15}$$

where $\gamma_c = Tc/(2L)$ characterizes the decay of the cavity and $\omega_{\rm FSR} = \pi c/L$ is the free spectral range of the cavity. This implies that the optical cavity plays the role of a microwave resonator for the microwave radiation imprinted on the pump light.

If the input light has two equal sidebands E_{+1} and E_{-1}, not a single sideband, the beat-note transforms as

$$\begin{aligned} &E^*_{\rm out}(t)E_{+1\ out}(t) + E^*_{-1\ out}(t)E_{\rm out}(t) \\ &= -\frac{T^2 E^*_{\rm in} E_{+1} e^{-i\omega_M t} e^{i\Delta\omega_M L/c}}{\left[1 - e^{-2i\Delta\omega_0 L/c}(1-T)\right]\left[1 - e^{2i(\Delta\omega_0 + \Delta\omega_M)L/c}(1-T)\right]} \\ &\quad - \frac{T^2 E^*_{-1} E_{\rm in} e^{-i\omega_M t} e^{i\Delta\omega_M L/c}}{\left[1 - e^{2i\Delta\omega_0 L/c}(1-T)\right]\left[1 - e^{-2i(\Delta\omega_0 - \Delta\omega_M)L/c}(1-T)\right]}. \end{aligned} \tag{16}$$

It follows from (16) that the beat-notes between each sideband and the carrier are transformed in the same way by the cavity.

Finally, it is worth noting that an ultra-high-Q cavity leads to the transfer of frequency fluctuations of the pump laser into the microwave signal if the bandwidth of the laser is comparable with γ_c. The slow light element discussed below does not have such a deficiency due to the pure two-photon nature of the process [11]. One may observe a narrow EIT peak with a wide bandwidth laser, which should be less than the Doppler width of the optical atomic transitions.

B. An Atomic Cell

An OEO may be stabilized with an atomic vapor cell containing atoms with a suitable energy level structure. One of the best atomic level configurations for such a purpose, the so-called Λ scheme, is shown in Fig. 2(b).

Let us assume that the pump light E_0 is nearly resonant with $|a\rangle \rightarrow |b\rangle$ atomic transition. If the EOM is switched off and the sideband E_{+1} is absent, the pump propagating through the atomic cell experiences a small residual absorption. The resonant absorption is suppressed due to optical pumping. For the pump amplitude we have (see the Appendix)

$$E_{\rm out}(t) \simeq E_{\rm in}\exp(-i\omega_0 t)\left(1 - \frac{\mathcal{N}\hbar\omega_0\gamma_0}{P_{\rm in}}\right)^{1/2} \tag{17}$$

where γ_0 is the decay rate of the ground state atomic coherence due to the finite interaction time of the atoms with light, $\mathcal{N}$ is the total number of atoms in the interaction region, and $P_{\rm in}$ is the pump power. Equation (17) is valid for intense light, where the condition

$$\wp^2|E_{\rm in}|^2 \gg \hbar^2\gamma_0 W_D \tag{18}$$

is fulfilled. Here $\wp$ is the value of dipole moment of the atomic transition, $E_{\rm in}$ is the electric field amplitude, and W_D is the Doppler width of the atomic transition.

Equation (17) stays valid when light is modulated and a weak sideband E_{+1} ($|E_{\rm in}| \gg |E_{+1}|$), nearly resonant with $|a\rangle \rightarrow |c\rangle$ atomic transition, propagates along with the pump in the cell. The sideband, however, acquires a large phase shift if the modulation frequency is different from the frequency of the transition between levels $|b\rangle$ and $|c\rangle$ (ω_{bc})

$$\begin{aligned} E_{+1\ out}(t) \simeq &E_{+1}\exp\left[-i(\omega_0 + \omega_M)t\right] \\ &\times \exp\left(\frac{1}{2}\left[1 - 2i\frac{\omega_M - \omega_{bc}}{\gamma_0}\right]\right. \\ &\left.\times \ln\left[1 - \frac{\mathcal{N}\hbar\omega_0\gamma_0}{P_{\rm in}}\right]\right). \end{aligned} \tag{19}$$

We are interested in the time delay introduced by the medium in the beat-note of the pump and the sideband. For small absorption we find

$$\begin{aligned} E^*_{\rm out}(t)E_{+1\ out}(t) \approx &E^*_{\rm in}E_{+1}e^{-i\omega_M t} \\ &\times \exp\left(\left[1 - i\frac{\omega_M - \omega_{bc}}{\gamma_0}\right]\right. \\ &\left.\times \ln\left[1 - \frac{\mathcal{N}\hbar\omega_0\gamma_0}{P_{\rm in}}\right]\right). \end{aligned} \tag{20}$$

Assuming that $\mathcal{N}\hbar\omega_0\gamma_0 \simeq \xi P_{\rm in}$ (small, but finite, absorption $1 \gg \xi > 0$) and $2\gamma_0 \gg |\omega_M - \omega_{bc}|$, we may approximate the response function of the system as

$$F_{sl} \approx e^{-\xi}\left[\frac{\gamma_0}{\gamma_0 - i(\omega_M - \omega_{bc})}\right]^{\xi/2}. \tag{21}$$

We have considered the case of single-sideband modulated light. Light modulated by a conventional EOM, however, has two sidebands instead of one. The second, off-resonant, sideband will not be influenced by the atomic transition if the pump power is weak enough so the four wave mixing processes occurring in the system and the resulting sideband amplification may be neglected. This condition may be approximated as $3N\lambda^2 L\gamma/(8\pi\omega_M) \ll 1$[19], where N is the density of the atomic vapor, λ is the wavelength of the pump light, L is the length of the atomic cell, and γ is the natural width of the atomic transition. This gives us the maximum density of the atomic vapor feasible for this application. For $\lambda = 0.78\ \mu$m, $L = 1$ cm, $\gamma = 5.7$ MHz, and $\omega_M = 6.8$ GHz, we have $N \ll 5 \times 10^{13}$ cm^{-3}.

Using these estimates and (17), we derive the maximum optical pump power for which the above approximation works. For a laser beam diameter $D = 0.5$ cm, we find $\mathcal{N} = \pi D^2 LN/4 \ll 10^{13}$. Assuming a wide two-photon resonance $\gamma_0 = 10^5$ rad/s, and taking $\omega_0 = 2.5 \times 10^{15}$ rad/s, we obtain $P_{\rm in} \ll 250$ mW. On the other hand, taking into account that $W_D = 500$ MHz and $\wp^2 = 3\hbar\gamma c^3/(4\omega_0^3)$, we find from (18) that the smallest optical power for which the above EIT regime holds is approximately 4 mW. For smaller power the narrow resonance still exists, but the residual absorption increases compared with the theoretical value.

For the amplitude modulated light that initially has equal harmonics ($|E_{\pm 1}| = E_{+1}$), the beat-note signal after the three-level medium is

$$E^*_{\rm out}(t)E_{+1\ out}(t) + E^*_{-1\ out}(t)E_{\rm out}(t) \approx E^*_{\rm in}E_{+1}\left(1-\frac{\mathcal{N}\hbar\omega_0\gamma_0}{P_{\rm in}}\right)^{1/2} e^{-i\omega_M t} \times\left\{1+\exp\left(\frac{1}{2}\left[1-2i\frac{\omega_M-\omega_{bc}}{\gamma_0}\right]\ln\left[1-\frac{\mathcal{N}\hbar\omega_0\gamma_0}{P_{\rm in}}\right]\right)\right\}. \quad (22)$$

The medium changes not only the phase of the beat-note but also its amplitude.

To avoid the difficulties arising from the asymmetry of the pump and sideband radiation mentioned above, one may use laser light modulated with half-frequency $\omega_M/2$ with respect to the ground state splitting of the atoms [18]. In this case the sidebands E_{+1} and E_{-1} interact with atoms via an effect of EIT, while the carrier $E_{\rm in}$ experiences a slight off-resonant absorption only. The beat-note in this case is

$$E^*_{\rm out}(t)E_{+1\ out}(t) + E^*_{-1\ out}(t)E_{out}(t) \approx (E^*_{\rm in}E_{+1} + E^*_{-1}E_{\rm in})e^{-i\omega_M t/2} \times\exp\left(\frac{1}{2}\left[1-i\frac{\omega_M-\omega_{bc}}{\gamma_0}\right]\ln\left[1-\frac{\mathcal{N}\hbar\omega_0\gamma_0}{P_{+1}+P_{-1}}\right]\right) \quad (23)$$

where P_{+1} and P_{-1} ($P_{+1}\simeq P_{-1}$) are the powers of the sidebands of the modulated light.

The chief advantage of this configuration is the (almost) complete symmetry, which allows for the reduction of the ac-Stark and other unwanted effects. Another advantage is that the four-wave mixing process, resulting from the scattering of the drive field on the atomic coherence generated by the sidebands, is not important in the scheme. The four-wave mixing leads to the generation of radiation with frequency $\omega_0 \pm \omega_M$. The beat-note originating from this process may be filtered out.

V. Characteristics of an Optoelectronic Oscillator With a Photonic Filter

Let us consider the scheme of an ideal OEO shown in Fig. 1(b). The amplitude and frequency of such an oscillator may be determined from (7)

$$\widetilde{E}_M = G\frac{\mathcal{A}cn}{2\pi}(E^*_d E_{+1\ d} + E^*_{-1\ d}E_d)\Big|_{\omega_M} e^{i\omega_M t} \quad (24)$$

where E_d and $E_{\pm 1\ d}$ are the complex amplitudes of the carrier and sidebands on the photodiode. Expressions for the oscillation frequency are quite complicated generally, so we consider the symmetric cases here.

A. Oscillation Amplitude

The oscillation amplitude for filters described by either (23) or (16) may be found from the real part of (24), which has the form

$$|\widetilde{E}_M| = \frac{1}{4}GP_{\rm in}\widetilde{\alpha}|\sin(\omega_0\tau_B)|\omega_0\widetilde{\tau}_M\left(1-\frac{1}{2}\omega_0^2\widetilde{\tau}_M^2\right) \quad (25)$$

where $\widetilde{\alpha}$ stands for the total transmission of the beat-note in the system and $\widetilde{\tau}_M = \xi L_S n_0^3 r_{\rm eff}|\widetilde{E}_M|/(2c)$.

B. Oscillation Frequency

The oscillation frequency may be found from the imaginary part of (24). For the atomic cell filter having a response according to (23), the oscillation frequency may be found from

$$\left(\frac{\omega_M}{2}-\omega_f\right)\tau_f - \frac{\omega_M-\omega_{bc}}{2\gamma_0}\ln\left[1-\frac{\mathcal{N}\hbar\omega_0\gamma_0}{P_{+1}+P_{-1}}\right] = 2\pi m + \zeta\pi \quad (26a)$$

where ζ is either unity if $\sin(\omega_0\tau_B) > 0$ or zero if $\sin(\omega_0\tau_B) < 0$; m is an integer number; ω_f is an eigenfrequency of the optical-microwave loop ($\omega_f\tau_f = 2\pi k$, where k is integer); and τ_f is determined by (9). Equation (26) means that the microwave field is a mode of an OEO loop, i.e., its cycle phase increment is integer multiple of 2π.

Note that in the "asymmetric" case, for example, when one sideband is off-resonant with the atomic transition, the oscillation frequency depends on the balance of the modulator (relative phase between the carrier and the harmonics). This happens because the medium shifts the phase of one harmonic, while leaving the other unchanged.

For the cavity filter described by (16) the frequency is determined by

$$(\omega_M-\omega_f)\tau_f + \frac{\omega_M-\omega_{\rm FSR}}{\gamma_c} = 2\pi m + \zeta\pi \quad (26)$$

where ζ is either one if $\sin(\omega_0\tau_B) < 0$ or zero if $\sin(\omega_0\tau_B) > 0$.

C. Oscillation Stability

To find the fluctuations of phase for the system, we replace (24) by

$$\widetilde{E}_M e^{-i\omega_M t} = G\gamma_G\int_0^t dt' P_d(t')e^{-(\gamma_G+i\omega_M)(t-t')} \quad (27)$$

where $\gamma_G \ll \omega_M$ is a filter bandwidth determined by the photodiode, for instance, and P_d is the total power of the modulated light at the photodiode. Noting that each field may be presented as a sum of the expectation and fluctuation parts ($E = \langle E\rangle + e$) and that the frequency of the microwave field may be written as $\omega_M + \delta\dot{\phi}(t)$, where $\delta\phi(t)$ is a slow function of time, we arrive at

$$\delta\dot{\phi}(t)\tilde{\tau} = \frac{i(e_M(t)-e^*_M(t))}{2|\langle E_M\rangle|} + \frac{G\gamma_G}{|\langle E_M\rangle|}\int_0^t dt' e^{-\gamma_G(t-t')}\sin(\omega_M t')\delta P_d(t') \quad (28)$$

where $\widetilde{\tau} = \tau_f - (\gamma_0)^{-1}\ln[1-(\mathcal{N}\hbar\omega_0\gamma_0)/(P_{+1}+P_{-1})]$ for an OEO with an atomic cell filter and $\tilde{\tau} = \tau_f + \gamma_c^{-1}$ for an OEO with a cavity filter.

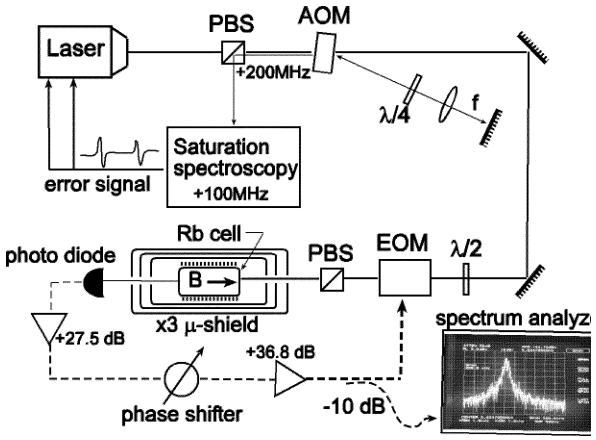

Fig. 3. Experimental setup for demonstration of the EIT-stabilized OEO.

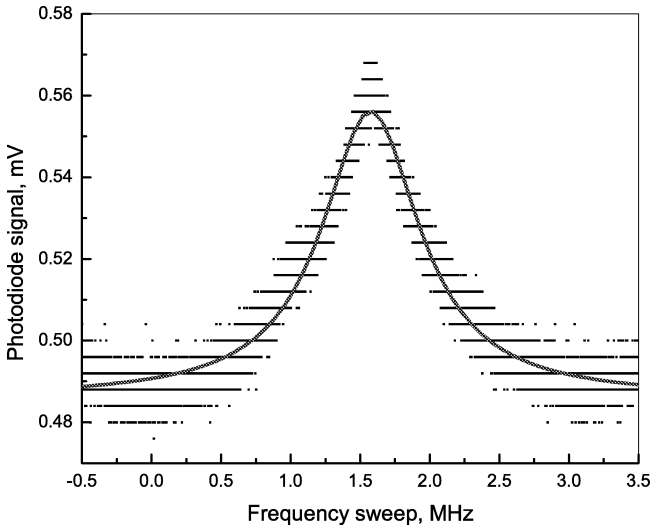

Fig. 4. The EIT peak observed in the transmission of the total signal. The data points line up due to limiting digitizing precision.

Assuming that the light, as well as the microwave, field is in a coherent state, we write a generic expression for the nonzero field moments

$$\langle e(t)e^*(t')\rangle = \frac{2\pi\hbar\omega}{\mathcal{A}c}\delta(t-t'). \tag{29}$$

Introducing the phase diffusion coefficient D as $\langle\delta\phi(t)^2\rangle - \langle\delta\phi(t)\rangle^2 = 2Dt$ and assuming that the time of the measurement is much longer than the filter characteristic time $1/\gamma_G$, we arrive at

$$D = (2\widetilde{\tau})^{-2}\left(\frac{\hbar\omega_M}{2\langle P_M\rangle} + \frac{4}{\omega_0^2\widetilde{\tau}_M^2}\frac{\hbar\omega_0}{\langle P_d\rangle}\right) \tag{30}$$

where we took $1 \gg \omega_0\widetilde{\tau}_M$ and $|\sin(\omega_0\tau_B)| = 1$, so that $G\langle P_d\rangle/|\langle E_M\rangle| \simeq \omega_0\widetilde{\tau}_M/2$, as follows from (25).

Finally, it is worth noting that the root mean square fractional frequency fluctuations for the oscillator may be found from the expression $\sigma_{\omega_M}/\omega_M = (2D/\omega_M^2 t)^{1/2}$, where t is the measurement time. It is clear that the frequency dispersion σ_{ω_M} is much less than the inverse effective delay time $\widetilde{\tau}$, which agrees with our experimental results discussed below.

VI. Experiment

We have demonstrated the operation of an OEO with a rubidium atomic cell serving as the stabilizing filter. The experimental setup of the EIT-stabilized OEO is shown in Fig. 3. We use a Vortex laser system tuned to the $5S_{1/2}$, $F = 2 \rightarrow 5P_{1/2}$, $F = 1$ transition of ^{87}Rb. This transition corresponds to transition $|a\rangle \rightarrow |b\rangle$ in Fig. 2(a). Then the transition $5S_{1/2}$, $F = 1 \rightarrow 5P_{1/2}$, $F = 1$ plays the role of $|a\rangle \rightarrow |c\rangle$. Transition frequencies differ by 6.834 68 GHz, which corresponds to ω_{bc} in Fig. 2(a).

The dual-pass acoustooptical modulator and a standard saturation spectroscopy setup allow us to lock the pump laser with approximately 300 MHz offset to the red from the $|a\rangle \rightarrow |b\rangle$ transition. This detuning turned out to be the optimal for the OEO operation of our system. We believe that the main factor determining this detuning value is the optimum dispersion/absorption ratio in the rubidium cell. This provides enough light for our OEO feedback loop to have the above-unity gain and enough dispersion to lock the OEO frequency to the atomic transition.

The laser light passes through an EOM, which, in combination with a rotating half-wave plate and a polarizer, allows the transforming of phase modulation into amplitude modulation. This conversion is important because in the case of pure phase modulation, no beat-note appears on a photodiode ($\sin(\tau_B\omega_0) = 0$). The beat signal produced with one sideband and the carrier has the opposite phase to the beat signal produced by the other sideband and the carrier, so they cancel out.

The amplitude-modulated light is then passed through a rubidium cell. The 2-in-long cell contains a natural abundance of rubidium isotopes at about 105 °C. The cell is placed inside of a solenoid, which is used to create a magnetic field along the propagation direction of the optical beam. The solenoid and the cell are enclosed in a three-layer μ-metal shield to cancel stray magnetic fields.

Light that passes through the cell is detected by a fast photodiode, the electric output of which is amplified and used to drive the EOM. Part of this microwave signal is directed to a spectrum analyzer to monitor the oscillation amplitude and frequency. A phase shifter is inserted into the circuit to achieve the desired microwave phase delay, which is an important condition for self-sustained oscillations.

As the first step in setting up the OEO oscillation, we open the feedback loop between the photodiode and the amplifiers, and drive the EOM with an RF synthesizer. Sweeping the synthesizer's frequency and detecting the signal from the photodiode, we obtained the frequency response functions of the system.

This is done in two different ways. First, we monitor the integrated signal from the photodiode, which corresponded to the total power of the light transmitted through the cell. When the external modulation frequency matches the hyperfine splitting frequency, we expect to see a higher transmission because of the EIT. The experimental result is shown in Fig. 4. We see the expected transparency peak; however, the contrast is rather poor. This is due to the fact that we are detecting an incremental increase of a sideband transmission, on the order of 10%, against

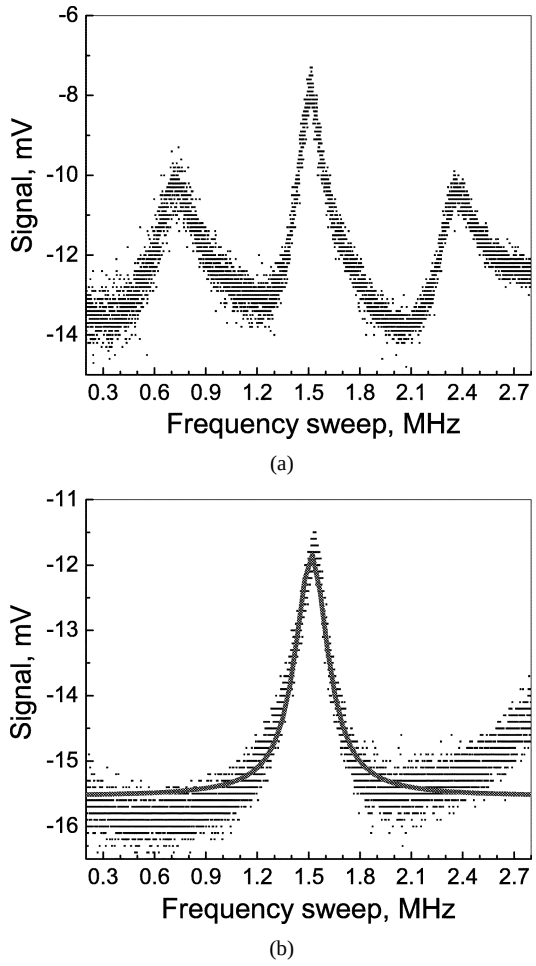

Fig. 5. Heterodyne signal as a function of the synthesizer frequency modulation. When the magnetic field is weak (on the left), peaks corresponding to transitions between different Zeeman levels are visible; when the field is strong (on the right), only the $m_1 = 0 \rightarrow m_2 = 0$ peak is present.

a much stronger carrier (by more than a factor of ten). Fitting the data with a Lorentzian peak function, we find its width to be approximately 860 kHz. This is a rather crude estimate for our filter function because of the low resolution of the peak and because the Lorentzian does not fit the EIT peak well.

A more accurate measurement is achieved by mixing the photodiode signal with the local oscillator signal obtained from the synthesizer driving the EOM, i.e., by implementing a heterodyne measurement. As part of this measurement, we subsequently turn on a dc magnetic field along the cell. The Zeeman shifts of magnetic sublevels m_F have opposite signs for $F = 1$ and $F = 2$, and hence for sufficiently large field all, transitions from the $F = 1 \rightarrow F = 2$ manifold are tuned off the two-photon resonance, except for the clock transition $m_1 = 0 \rightarrow m_2 = 0$.

The measurement results are shown in Fig. 5. On the top part of the figure [Fig. 5(a)], the magnetic field is small, and in addition to the central peak $m_1 = 0 \rightarrow m_2 = 0$, we see two other peaks. On the bottom part [Fig. 5(b)], the field is strong (several Gauss), and the side peaks have moved far outside the sweep range. Such a strong magnetic field is on in all the experiments described below. Fitting the single peak to a Lorentzian, we find its width to be approximately 230 kHz.

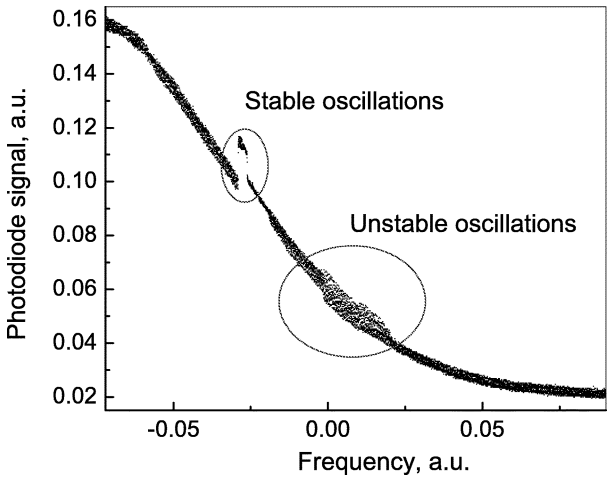

Fig. 6. Rubidium cell transmission signal on the red wing of Doppler broadened line. Irregular segments indicate the ranges of OEO oscillations.

Next, we remove the synthesizer and connect the photodiode to the amplifiers, closing the feedback loop. Two distinct regimes of RF oscillation have been observed. Outside the EIT region, the system can oscillate at any frequency within 100-MHz range. This range is determined by the bandwidth of the EOM and of the RF amplifiers, and the frequency can be tuned by the phase shifter.

When the EIT condition is achieved, the oscillation frequency is locked at the atomic hyperfine transition frequency. By a suitable choice of the experimental parameters, this desired oscillation can suppress the other, broadly tunable type. This EIT-stabilized regime can be achieved only within a fairly narrow range of the laser wavelength.

To illustrate the effect of laser wavelength tuning on the OEO operation, we slowly scanned the wavelength while measuring the integrated photodiode signal. The result is given in Fig. 6. In this figure the red slope of Doppler absorption profile is shown. The entire scan is approximately 700–800 MHz wide. We see two wavelength ranges where oscillations occur: the one on the red side corresponds to stable oscillation and is manifested by a higher transmission (due to EIT); the one on the blue side corresponds to unstable oscillations and is manifested by higher noise.

Drift of the laser wavelength within the EIT-stabilized region causes the microwave phase to change, which needs to be compensated by the phase shifter. It therefore appears convenient to lock the laser near the center of the desired wavelength range. However, the nature of laser locking by the frequency-modulated saturation spectroscopy [20]–[22] imposes additional structure on the microwave oscillation spectrum; see Fig. 7. The peaks in this figure are separated by approximately 28 kHz from each other. This frequency is the dither frequency of the laser lock. It worth noting that this structure may disappear if the laser is not modulated directly.

Unlocking the laser, we get rid of the 28-kHz structure and observe a single peak, which is quite narrow. From Fig. 8, we see that its width is approximately 1 kHz. It is important to point out that this width is much narrower than the EIT width, which is consistent with (30). The peak in Fig. 8 can drift within approximately ± 500 kHz before the oscillations become unstable and

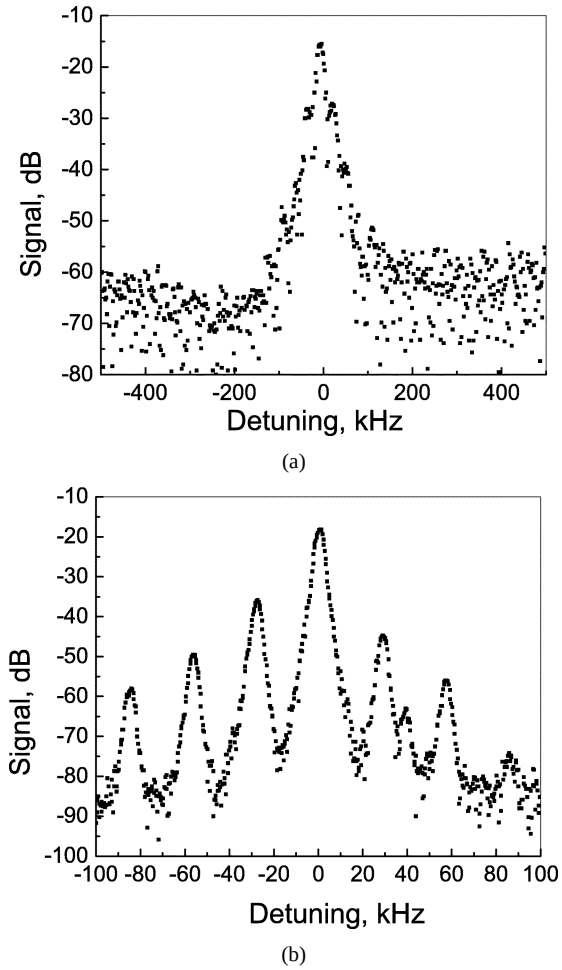

Fig. 7. (a) Microwave oscillation spectrum for the OEO with locked laser. (b) The same, with higher resolution. The zero detuning corresponds to the hyperfine transition frequency $\omega_M \approx 6.8$ GHz. The peaks are separated by 28 kHz, the dither frequency of the FM spectroscopy laser lock, that imposes additional modulation on the laser light.

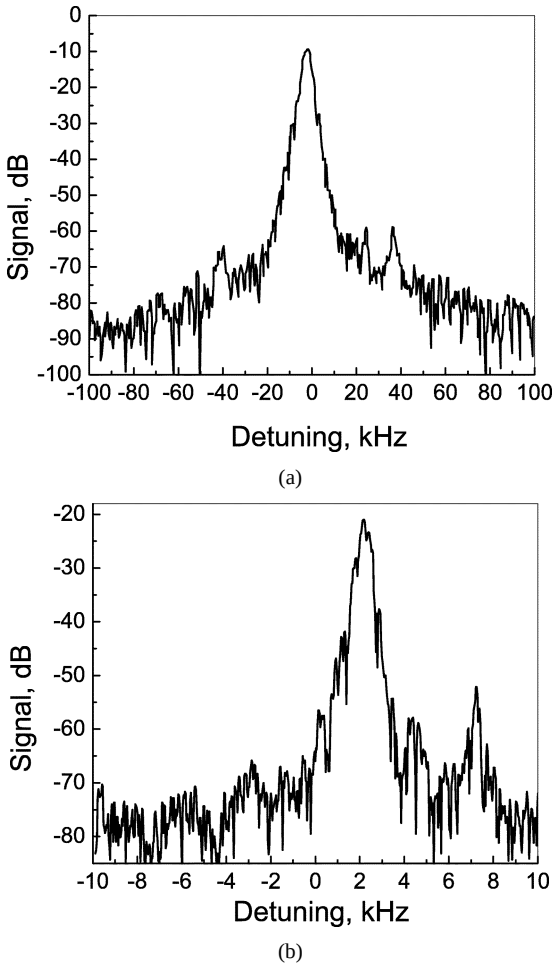

Fig. 8. (a) The RF spectrum with a free-running laser; resolution is limited by the spectrum analyzer bandwidth. (b) The same with higher resolution, yielding the RF spectral width of approximately 1 kHz. The zero detuning corresponds to the hyperfine transition frequency $\omega_M \approx 6.8$ GHz.

disappear. This range is consistent with the EIT width measured by the first method. The situation can be improved by obtaining a narrower EIT signal. Note that this regime of operation is similar to that of the CPT clocks [18].

We also carried out an experiment in which both the rubidium cell and a 250-m fiber were present. This configuration represents an OEO with an atomic cell filter. Significantly, in this case the linewidth of the transition-locked oscillations was measured to be less than 100 Hz, while the tuning range remained the same as without the fiber.

Let us estimate theoretical value of σ_{ω_M} for the conditions of the experiment. To do it, we modify (30) as

$$D_A = (2\widetilde{\tau})^{-2}\left(\frac{(2G_A-1)\hbar\omega_M}{2\langle P_M\rangle} + \frac{4}{\omega_0^2\widetilde{\tau}_M^2}\frac{\hbar\omega_0}{\langle P_d\rangle}\right). \quad (31)$$

Equation (31) takes into account amplification of the microwave generated on a photodiode that was present in the experiment ($G_A \geq 1$ is the coefficient of the power amplification).

We assume that $\omega_M = 2\times 10^{10}$ s^{-1}, $\widetilde{\tau} = 1$ μs, $P_M = 1$ W, $G_A = 2.7\times 10^6$, $P_d \simeq 10$ μW, $\omega_0 = 2\times 10^{15}$ s^{-1}. We know from the experiment that the ratio of the power of the sideband and carrier after the modulator is approximately 10%, i.e., from (3) and (4), $\omega_0^2\widetilde{\tau}_M^2/4 \simeq 0.1$. The measurement time was $t \approx 0.01$ s. Then, $\sigma_{\omega_M} = (2D_A/t)^{1/2} \simeq 3$ s^{-1}, which is approximately a hundred times smaller than the observed linewidth.

The phase diffusion parameter D_A determines the phase noise of the generated microwaves. In our experiment, this parameter was four orders of magnitude in excess of the shot noise limit given by (31). This difference may appear because of the technical noise such as the pump laser excess noise and temperature fluctuations. In the present proof-of-principle experiment, we did not make any efforts to suppress these sources of noise.

VII. Discussion

Let us compare properties of the photonic filters discussed in this paper. Both filters are similar in the sense that they have higher transmission of modulated light when the frequency of the modulation coincides with an intrinsic frequency of the filter—either frequency of the free spectral range of the cavity or frequency of the splitting between atomic ground states.

The main differences between an atomic cell containing a vapor of three-level atoms and a high-Q optical cavity are the following.

1) An ideal cavity transmits modulated light without absorption if the carrier frequency of the light coincides with a cavity mode and the modulation frequency coincides with the free spectral range frequency of the cavity. The transmission does not depend on the cavity quality factor. In turn, the atomic cell absorbs passing modulated light. The maximum transmission, achieved when the modulation frequency of the light coincides with the frequency of the ground state splitting of the atoms, is connected with the width of the two-photon resonance.
2) The frequency of the cavity drifts depending on the external conditions while the splitting of the atomic ground state may be stable. Hence, usage of an atomic cell instead of a cavity is useful for construction of frequency references.
3) An atomic cell is more tolerant to the absolute pump laser stability compared to a cavity. If light having wide linewidth propagates through a high-Q cavity, the phase fluctuations of the input light are transmitted to the amplitude fluctuations of the outgoing light. Such a transfer influences the stability of oscillations in the entire system. In turn, linewidth of the pump light used in an OEO with an atomic cell is determined by the width of the atomic spectral line and may be much wider than the width of the two-photon resonance, which is used for OEO stabilization.

It is worth noting here that an optical fiber plays not only the role of the microwave cavity in the OEO but also the role of a filter, see e.g., (26a) and (26). Generally, it is possible to make a very long fiber delay in an OEO. Then the OEO generates several harmonics with linewidth determined by the fiber length. The number of harmonics is restricted by a linewidth of a photonic filter used in the system.

VIII. Conclusion

In this paper, we have theoretically studied the properties of an optoelectronic oscillator realized with photonic filters such as a high-Q optical cavity and an atomic vapor cell. We show that the oscillator is able to generate stable microwave signals at a frequency determined by the filter. We also report an experimental demonstration of an OEO stabilized with an Rb atomic vapor cell. Because such a device can be miniaturized and has a potentially high stability, this paper is a step toward the creation of a miniature frequency reference.

Appendix
EIT and Slow Light

Let us consider the interaction of the electromagnetic waves with atomic vapor confined in a vapor cell [Fig. 2(b)]. The stationary propagations of light through the cell is described by Maxwell equations in the slowly varying amplitude and phase approximation

$$\frac{\partial}{\partial z}E_0(z) = \frac{2i\pi\omega_0}{c}\wp_{ab}N\rho_{ab} \tag{32}$$

$$\frac{\partial}{\partial z}E_{+1}(z) = \frac{2i\pi\omega_0}{c}\wp_{ac}N\rho_{ac} \tag{33}$$

where N is the atomic number density, $\wp_{ab}$ and $\wp_{ac}$ are the dipole moments of the respective transitions, and ρ_{ab} and ρ_{ac} are the density matrix elements of the corresponding atomic transitions. Analytic expressions for the matrix elements can be obtained from the stationary solution of the c-number equations [8], [11]

$$\begin{aligned}
\dot\rho_{bb} &= \frac{\gamma_0}{2} - \gamma_0\rho_{bb} + \gamma\rho_{aa} + i(\Omega_0^*\rho_{ab} - c.c.)\\
\dot\rho_{cc} &= \frac{\gamma_0}{2} - \gamma_0\rho_{cc} + \gamma\rho_{aa} + i(\Omega_{+1}^*\rho_{ac} - c.c.)\\
\dot\rho_{bc} &= -\Gamma_{bc}\rho_{bc} + i\Omega_0^*\rho_{ac} - i\Omega_{+1}\rho_{ba}\\
\dot\rho_{ab} &= -\Gamma_{ab}\rho_{ab} + i\Omega_0(\rho_{bb} - \rho_{aa}) + i\Omega_{+1}\rho_{cb}\\
\dot\rho_{ac} &= -\Gamma_{ac}\rho_{ac} + i\Omega_{+1}(\rho_{cc} - \rho_{aa}) + i\Omega_0\rho_{bc}
\end{aligned}$$

where

$$\begin{aligned}
\Gamma_{ab} &\simeq \gamma + i\delta\\
\Gamma_{ac} &\simeq \gamma - i\delta\\
\Gamma_{cb} &\simeq \gamma_0 + 2i\delta.
\end{aligned}$$

$2\delta = \omega_M - \omega_{bc}$, $\Omega_0 = \wp_{ab}E_0/\hbar$, and $\Omega_{+1} = \wp_{ac}E_{+1}/\hbar$ are the Rabi frequencies, and $\rho_{aa} + \rho_{bb} + \rho_{cc} = 1$.

We calculate the stationary solutions of the equations by considering only the lowest order in γ_0 and δ

$$\frac{\partial}{\partial z}\Omega_0 = -\frac{3}{8\pi}N\lambda^2\gamma\frac{\Omega_0}{|\Omega|^4}\left(\frac{\gamma_0}{2}|\Omega|^2 + 2i\delta|\Omega_{+1}|^2\right) \tag{34}$$

$$\frac{\partial}{\partial z}\Omega_{+1} = -\frac{3}{8\pi}N\lambda^2\gamma\frac{\Omega_{+1}}{|\Omega|^4}\left(\frac{\gamma_0}{2}|\Omega|^2 - 2i\delta|\Omega_0|^2\right) \tag{35}$$

where $|\Omega|^2 = |\Omega_0|^2 + |\Omega_{+1}|^2$. Then

$$\frac{\partial}{\partial z}|\Omega|^2 \simeq -\frac{3}{8\pi}N\lambda^2\gamma_0\gamma. \tag{36}$$

Assuming that $|\Omega_0|^2 \gg |\Omega_{+1}|^2$, we derive

$$|\Omega_0(z)|^2 = |\Omega_0(0)|^2\left(1 - \frac{3}{8\pi}N\lambda^2\frac{\gamma_0\gamma}{|\Omega_0(0)|^2}z\right) \tag{37}$$

$$\frac{\partial}{\partial z}\Omega_{+1} = -\frac{3}{8\pi}N\lambda^2\gamma\frac{\Omega_{+1}}{|\Omega_0|^2}\left(\frac{\gamma_0}{2} - 2i\delta\right). \tag{38}$$

Equation (17) may be derived from (37) and (19) may be derived from (38), if one takes into account that $\wp^2 = 3\hbar\gamma c^3/(4\omega_0^3)$, $|E|^2 = 2\pi P/\mathcal{A}c$, and $\mathcal{N} = NL\mathcal{A}$.

References

[1] X. S. Yao and L. Maleki, "Optoelectronic microwave oscillator," *J. Opt. Soc. Amer. B*, vol. 13, pp. 1725–1735, 1996.

[2] Y. Ji, X. S. Yao, and L. Maleki, "Compact optoelectronic oscillator with ultralow phase noise performance," *Electron. Lett.*, vol. 35, pp. 1554–1555, 1999.

[3] T. Davidson, P. Goldgeier, G. Eisenstein, and M. Orenstein, "High spectral purity CW oscillation and pulse generation in optoelectronic microwave oscillator," *Electron. Lett.*, vol. 35, pp. 1260–1261, 1999.

[4] S. Romisch, J. Kitching, E. Ferre-Pikal, L. Hollberg, and F. L. Walls, "Performance evaluation of an optoelectronic oscillator," *IEEE Trans. Ultrason. Ferroelect. Freq. Contr.*, vol. 47, pp. 1159–1165, 2000.

[5] X. S. Yao and L. Maleki, "Multiloop optoelectronic oscillator," *IEEE J. Quantum Electron.*, vol. 36, pp. 79–84, 2000.

[6] S. Poinsot, H. Porte, J. P. Goedgebuer, W. T. Rhodes, and B. Boussert, "Continuous radio-frequency tuning of an optoelectronic oscillator with dispersive feedback," *Opt. Lett.*, vol. 27, pp. 1300–1302, 2002.

[7] D. H. Chang, H. R. Fetterman, H. Erlig, H. Zhang, M. C. Oh, C. Zhang, and W. H. Steier, "39-GHz optoelectronic oscillator using broad-band polymer electrooptic modulator," *IEEE Photon. Technol. Lett.*, vol. 14, pp. 191–193, 2002.

[8] E. Arimondo, "Coherent population trapping in laser spectroscopy," *Progress Opt.*, vol. 35, pp. 257–354, 1996.

[9] S. E. Harris, "Electromagnetically induced transparency," *Phys. Today*, vol. 50, pp. 36–42, 1997.
[10] J. P. Marangos, "Topical review on electromagnetically induced transparency," *J. Mod. Opt.*, vol. 45, pp. 471–503, 1998.
[11] A. B. Matsko, O. Kocharovskaya, Y. Rostovtsev, G. R. Welch, A. S. Zibrov, and M. O. Scully, "Slow, ultraslow, stored, and frozen light," *Adv. At. Mol. Opt. Phys.*, vol. 46, p. 191, 2001.
[12] R. W. Boyd and D. J. Gauther, "Slow and fast light," *Progress Opt.*, vol. 43, pp. 497–530, 2002.
[13] L. V. Hau, S. E. Harris, Z. Dutton, and C. H. Behroozi, "Light speed reduction to 17 meters per second in an ultracold atomic gas," *Nature*, vol. 397, pp. 594–598, 1999.
[14] M. M. Kash, V. A. Sautenkov, A. S. Zibrov, L. Hollberg, G. R. Welch, M. D. Lukin, Y. Rostovtsev, E. S. Fry, and M. O. Scully, "Ultraslow group velocity and enhanced nonlinear optical effects in a coherently driven hot atomic gas," *Phys. Rev. Lett.*, vol. 82, pp. 5229–5232, 1999.
[15] D. Budker, D. Kimball, S. Rochester, and V. Yashchuk, "Nonlinear magneto-optics and reduced group velocity of light in atomic vapor with slow ground state relaxation," *Phys. Rev. Lett.*, vol. 83, pp. 1767–1770, 1999.
[16] A. V. Turukhin, V. S. Sudarshanam, M. S. Shahriar, J. A. Musser, B. S. Ham, and P. R. Hemmer, "Observation of ultraslow and stored light pulses in a solid," *Phys. Rev. Lett.*, vol. 88, p. 023 602, 2002.
[17] M. S. Bigelow, N. N. Lepeshkin, and R. W. Boyd, "Observation of ultrasolw light propagation in a ruby crystal at room temperature," *Phys. Rev. Lett.*, vol. 90, p. 113 903, 2003.
[18] J. Kitching, S. Knappe, and L. Hollberg, "Miniature vapor-cell atomic-frequency references," *Appl. Phys. Lett.*, vol. 81, pp. 553–555, 2002.
[19] M. D. Lukin, M. Fleischhauer, A. S. Zibrov, H. G. Robinson, V. L. Velichansky, L. Hollberg, and M. O. Scully, "Spectroscopy of dense coherent media: Line narrowing and interference effects," *Phys. Rev. Lett.*, vol. 79, pp. 2959–2963, 1999.
[20] J. M. Supplee, E. A. Wittaker, and W. Lenth, "Theoretical description of frequency modulation and wavelength modulation spectroscopy," *Appl. Opt.*, vol. 33, pp. 6294–6302, 1994.
[21] J. L. Hall, L. Hollberg, T. Baer, and H. G. Robinson, "Optical heterodyne saturation spectroscopy," *Appl. Phys. Lett.*, vol. 39, pp. 680–682, 1981.
[22] S. Kasapi, S. Lathi, and Y. Yamamoto, "Amplitude-squeezed, frequency-modulated, tunable, diode-laser-based source for sub-shot-noise FM spectroscopy," *Opt. Lett.*, vol. 22, pp. 478–480, 1997.

Dmitry Strekalov received the B.S. and M.S. degrees from Moscow State University, Moscow, Russia, in 1992 and 1994, respectively, and the Ph.D. degree from the University of Maryland, Baltimore County, in 1997.

He received postdoctoral training from 1997 to 1999 at the Physics Department, New York University, and from 1999 to 2000, at the Physics Department, Rice University, Houston, TX. He joined the Jet Propulsion Laboratory (JPL), California Institute of Technology, Pasadena, in 2000, where he is currently a Senior Staff Member of the Quantum Science and Technology. He has more than 20 publications in peer-reviewed physics journals, with the cumulative citation index over 285. The majority of these works are experimental research in quantum optics (photon entanglement; quantum-optical interference, diffraction, and imaging; and tests of Bell's inequalities) and in atomic optics (cooling and trapping of atoms, BEC, Raman spectroscopy, coherent atomic systems, and slow light), which is the current area of his research.

Dr. Strekalov was awarded the Robert A. Welch Foundation Postdoctoral Fellowship at Rice University in 1999, and in 2002, he received JPL's Lew Allen Award for excellence.

David Aveline received the B.S. degree in applied and engineering physics (*cum laude*) from Cornell University, Ithaca, NY, in 2002.

He joined the Quantum Sciences and Technology group at the Jet Propulsion Laboratory (JPL), California Insitute of Technology, Pasadena, as a Member of Engineering Staff. He has been active in the field of laser cooling and atomic physics at JPL, including research in the areas of Bose–Einstein condensation, electromagnetically induced transparency, atom-wave interferometry, and laser technology development. He has also been involved with environmental and biological research at the University of Rhode Island and Rhode Island College.

Mr. Aveline is a Member of the American Physical Society and the Optical Society of America (OSA).

Nan Yu received the B.S. degree from the Nanjing Institute of Technology, Nanjing, China, in 1982 and the M.S. and Ph.D degrees in physics from the University of Arizona, Tucson, in 1985 and 1988, respectively.

After several years as a Postdoctoral Research Associate, he joined the research faculty at the University of Washington, Seattle, and carried out research work in the areas of single ion trapping, laser cooling, and high-resolution spectroscopy. In 1998, he joined the Jet Propulsion Laboratory, California Institute of Technology, Pasadena, as a Senior Member of Technical Staff. His research interests include trapping and cooling ions and neutral atoms, atom interferometer for inertial sensing, photonic generation of ultra-low-phase-noise microwave signal and optical pulses, and development of novel frequency standard and atomic clocks.

Robert Thompson received the B.S. degree from the Georgia Institute of Technology, Atlanta, and the Ph.D. degree from the University of Texas in 1985 and 1994, respectively.

He is a Senior Member of Technical Staff with the Quantum Sciences and Technology group, Jet Propulsion Laboratory (JPL), Caifornia Institute of Technology, Pasadena. At JPL, he has been active in the field of laser cooling and atomic physics, including research in the areas of Bose–Einstein condensation, atomic waveguides, and laser technology development.

Dr. Thompson is a Member of the American Physical Society.

Andrey B. Matsko received the M.S. and Ph.D. degrees from Moscow State University, Moscow Russia, in 1994 and 1996, respectively.

He received postdoctoral training at the Department of Physics, Texas A&M University, from 1997 to 2001. He has been a Senior Member of Technical Staff with the Quantum Sciences and Technology group, Jet Propulsion Laboratory, California Institute of Technology, Pasadena, since 2001. His current research interests include, but are not restricted to, applications of whispering-gallery-mode resonators in quantum and nonlinear optics and photonics; coherence effects in resonant media; and quantum theory of measurements.

Dr. Matsko is a Member of the Optical Society of America (OSA). He was awarded the Robert A. Welch Foundation Postdoctoral Fellowship.

Lute Maleki (M'89–SM'96–F'00) is a Senior Research Scientist and the Supervisor of the Quantum Sciences and Technology group, Jet Propulsion Laboratory, California Institute of Technology, Pasadena. His current research includes the study and development of whispering-gallery-mode microresonators for photonics and quantum optics applications, including sensors and optoelectronic sources of optical and microwave reference frequencies. He is also active in the development of atomic clocks based on ions and neutral atoms, laser cooling and atomic physics for quantum control, and the development of sensors based on atom-wave interferometers. He is also active in tests of fundamental physics with ground- and space-based clocks.

Dr. Maleki is a Member of the American Physical Society and the Optical Society of America (OSA). He is the recipient of the IEEE I. I. Rabi Award for the development of clocks for space.